

Bridging Gaps in Laser Transmission Welding of Thermoplastics

James D. Van de Ven
e-mail: vandeven@me.umn.edu

Arthur G. Erdman
e-mail: agerdman@me.umn.edu

Mechanical Engineering Department,
University of Minnesota,
111 Church Street Southeast,
Minneapolis, MN 55455

Gaps at part interfaces pose a major challenge for laser transmission welding (LTW) of thermoplastics due to the reliance on contact conduction between the absorptive and transmissive parts. In industrial applications, gaps between parts can occur for a variety of tolerance and process control reasons. Previous experimental and modeling work in LTW has focused on gap-free joints, with little attention to bridging a gap with thermal expansion of the absorbing material. A two-dimensional comprehensive numerical model simulated bridging gaps in LTW. Using the model, operating parameters were selected for welding across a 12.7 μm gap and a 25.4 μm gap by creating sufficient thermal strain to bridge the gap and form a weld. Using these operating parameters, PVC samples were welded in a T-joint geometry with a designed gap. The quality of the welds was assessed visually, by destructive force testing and by measuring the weld size to quantify the weld strength. All the experimental samples, for the two gap sizes, bridged the gap and formed welds. The average weld strength of the 12.7 μm gap samples was 16.1 MPa, while the 25.4 μm gap samples had an average strength of 10.0 MPa. Gaps were successfully bridged with LTW by using a two-dimensional model to design the operating parameters. To achieve higher modeling accuracy, a three-dimensional model might better simulate the thermal diffusion in the direction of laser travel.

[DOI: 10.1115/1.2769731]

Keywords: laser welding, gap bridging, modeling, PVC

Background

Laser transmission welding (LTW) is a popular thermoplastic joining option because it is a contact-free operation that creates excellent quality welds. Due to a relatively large operating window for variation in process parameters, including weld velocity, laser power, and clamping pressure, LTW is a robust joining process from a manufacturing viewpoint [1–3]. One important process variable not previously explored in LTW is the presence of gaps in the joint.

Gaps occur in a joint for a variety of reasons including poor dimensional control of mating part features, inadequate clamping force, poor clamping location, warping, and poor joint design. The presence of gaps in LTW using the contour method is a major concern because the process relies on thermal contact conduction between the absorptive part and the transmissive part [2]. When these two parts are not in contact, conduction of the heat created by laser radiation will not occur across the part interface, causing the temperature of the absorptive part to rapidly increase. If the thermal expansion of the absorptive part does not create contact with the transmissive part and “bridge” the gap, thermal decomposition of the absorptive part will likely occur.

Very little previous work has investigated bridging gaps in LTW from either an experimental or a modeling approach. Russek et al. [4] briefly reports that bridging gaps is possible by increasing the optical penetration depth through changing the absorption coefficient of absorbing material. This work states that gaps up to 150 μm are bridgeable using a circular laser spot in contour welding [4]. It should be noted that simultaneous and quasisimulta-

neous variants of LTW create meltdown at the joint. Bridging gaps is not as significant of a challenge with these two variants of LTW as it is for the contour method.

Designing a laser transmission weld to bridge a gap requires careful consideration of the heating distribution. The absorbing part must be heated slowly to allow conduction into the bulk of the material, which will increase the thermal strain and allow the two parts to meet. Achieving the necessary thermal strain is not trivial because the thermal conductivity of polymers is relatively low and during a longer weld time, the possibility of thermal decomposition becomes greater.

This paper presents an investigation of bridging gaps in LTW of PVC using the contour method. Two different gap sizes will be discussed, 12.7 μm and 25.4 μm . Using a numerical model previously developed [2], simulations were run that design operating parameters for both gap sizes. Using the designed operating parameters, samples were welded and assessed for aesthetics, weld strength, and weld width.

Laser Transmission Welding Model Description

A comprehensive numerical model was developed from first principles of heat transfer and present in previous works [1–3]. This model uses the energy balance method to calculate the temperature at nodes in two dimensions: into the material (z direction) and perpendicular to the direction of laser travel (x direction). The model includes radiation from the material surfaces to the surroundings, convection from the external surfaces to the surrounding air, laser reflection from both surfaces, heat generation within each material from laser absorption, conduction within each material, and contact conduction between the two parts. A diagram explaining the heat transfer aspects of the model can be seen in Fig. 1.

In addition to calculating the temperature of each node, the model also calculates the joining pressure at the interface between the two parts. Initial clamping and thermal expansion during heat-

Contributed by the Manufacturing Engineering Division of ASME for publication in the JOURNAL OF MANUFACTURING SCIENCE AND ENGINEERING. Manuscript received November 3, 2006; final manuscript received July 6, 2007. Review conducted by Y. Lawrence Yao.

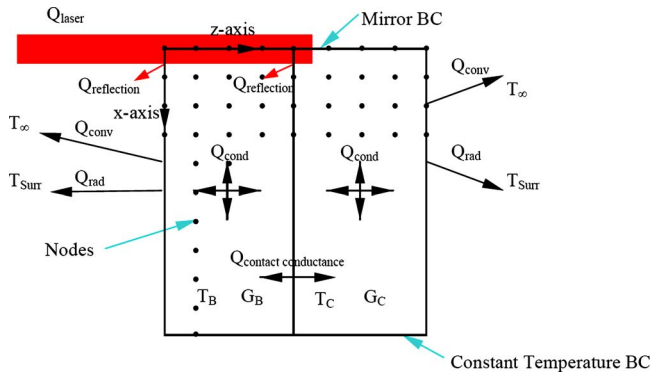


Fig. 1 This diagram shows the heat transfer components of the two-dimensional numerical model. Material B is the transmissive part and Material C is the absorptive part. In this view, the laser beam is collinear with the positive z axis and is traveling into the paper in the direction of the positive y axis (not labeled).

ing create this joining pressure. In the case of welding across a gap, the initial joining pressure is zero and only begins to rise after sufficient thermal expansion creates contact between the absorptive and transmissive parts.

The model also includes many advanced attributes including material properties that vary with temperature and pressure and a Gaussian laser distribution obtained from experimental measurements [1,2]. Material properties that vary with temperature include the specific volume [5], which allows the thermal expansion to be calculated, the absorption coefficient [6], the elastic modulus [7,8], the specific heat [8], and the thermal conductivity [8]. Additionally, the contact conduction varies with both temperature and joining pressure and warrants further discussion.

Contact conduction between the joined parts is vital to LTW, as is demonstrated most emphatically when evaluating gap bridging. A model developed based on microscopic elastic deformation allows the contact conduction to be expressed as follows:

$$h_c = \frac{1.49km_{ab}}{R} \left(\frac{2.3P}{Em_{ab}} \right)^{0.935} \quad (1)$$

where h_c is the contact conductance ($W/m^2 K$), k is the thermal conductivity ($W/m K$), m_{ab} is the mean asperity slope (rad), R is the root mean square of the surface roughness (m), P is the joining pressure (Pa), and E is the elastic modulus (Pa) [9]. This equation demonstrates that the pressure is nearly directly proportional to the contact conduction; without pressure, conduction does not occur. While it can be argued that convection and radiation do occur across a gap, these are not significant compared to conduction. High contact conduction is paramount to creating a successful LTW.

Modeling Gap Bridging

The described model is used to simulate LTW for two different gap sizes, $12.7 \mu m$ and $25.4 \mu m$, using the same part geometry. These gap sizes were selected as they sufficiently demonstrate the changes in process parameters necessary to bridge a gap within reasonable welding velocities and can be easily constructed with commercially available shims. The example joint consists of two $127 \text{ mm long} \times 25 \text{ mm wide} \times 3.2 \text{ mm thick}$ PVC parts with a surface roughness of $1.3 \mu m$; the absorptive part is gray in color and the transmissive part is clear. Both the clear and transparent parts are type I PVC from K-mac Plastics¹. The transmissive part will be placed above the gray part and fixtured such that a known

gap between the two parts is obtained. The radiation source is a fiber coupled diode laser operating at a wavelength of 808 nm with a maximum output power of 40 W .

The model is used in an iterative manner to achieve the desired weld characteristics by varying the process parameters as previously described [1,2]. To provide a match to previous work, the laser beam diameter is set to 5.7 mm . Through an iterative design process, the laser parameters selected to bridge a $12.7 \mu m$ (0.0005 in.) gap have a laser velocity of 0.0025 m/s (0.10 in./s) and a laser power of 2.5 W . For reference, when operating without a gap, an applied clamping pressure of 2 MPa and a beam diameter of 5.7 mm , the solution parameters were a weld velocity of 0.06 m/s and a laser power of 17 W , which created a 2.5 mm wide weld [1,2].

The resolution and computation speed of the model can be modified by adjusting the distance between the nodes within the materials, which changes the overall number of nodes, and by changing the time step. In simulating the $12.7 \mu m$ gap, the model is run for 2.3 s with a time step of 2 ms . The distance between each node is set to 0.05 mm . Selecting the time step and distance between nodes is a balance between processing time and accuracy while satisfying the stability criterion,

$$\tau = \frac{k\Delta t}{\rho C\Delta x^2} \leq \frac{1}{2} \quad (2)$$

where τ is the mesh Fourier number, Δt is the time step, ρ is the mass density, C is the specific heat, and Δx is the distance between nodes [10]. Output plots from the model for this design solution are presented in Figs. 2 and 3.

As can be seen in Fig. 2, a large amount of time elapses before the gap is closed and heating of the transmissive material begins. Even with a very low laser power of 2.5 W , the temperature within the absorptive material reaches over 786 K , which causes concern of thermal decomposition. The weld width predicted by the model is the width that exceeds a temperature of 485 K , which is most easily observed in the lower plot of Fig. 3. 485 K is set as the defining temperature of a weld from previous work welding PVC sheets with a heated pin [1,11]. The predicted weld width for this set of process parameters is 2.10 mm , markedly narrower than the 2.50 mm wide weld obtained when no gap was present and the laser beam was the same diameter.

Process parameters were also designed for a larger gap size of $25.4 \mu m$ (0.001 in.). As expected, a slower weld velocity is required to allow sufficient thermal expansion to bridge the larger gap. To avoid decomposing the polymer during longer weld times, the line energy, defined as the laser power divided by the laser velocity, needs to be decreased. The line energy is decreased by either decreasing the laser power or increasing the laser beam diameter. Below 2.5 W of power, the available diode laser significantly loses efficiency and the output power is more difficult to predict [12]. For this reason, an additional constraint added to this design is a desire to operate at or above 2.5 W . Using an iterative design method, suitable solution was found at the following operating parameters: a laser power of 2.5 W , a beam diameter of 8 mm , and a weld velocity of 0.001 m/s (0.039 in./s). Using a time step of 0.01 s and a distance between the nodes of 0.1 mm , the model produced the plots found in Figs. 4 and 5. The time step and distance between the nodes were increased from the earlier model to keep the processing manageable during the 9 s weld time.

It should be noted that welding across a significant gap requires a very slow welding velocity. This low velocity is needed to elevate the temperature through a considerable depth in the absorptive part, creating the needed thermal expansion to bridge the gap. This heating away from the weld zone can especially be observed in Fig. 5 where the temperature contour lines extend a significant distance in the depth direction from the part interface. The weld

¹K-mac Plastic, 3821 Clay Ave. SW, Wyoming, MI 49548.

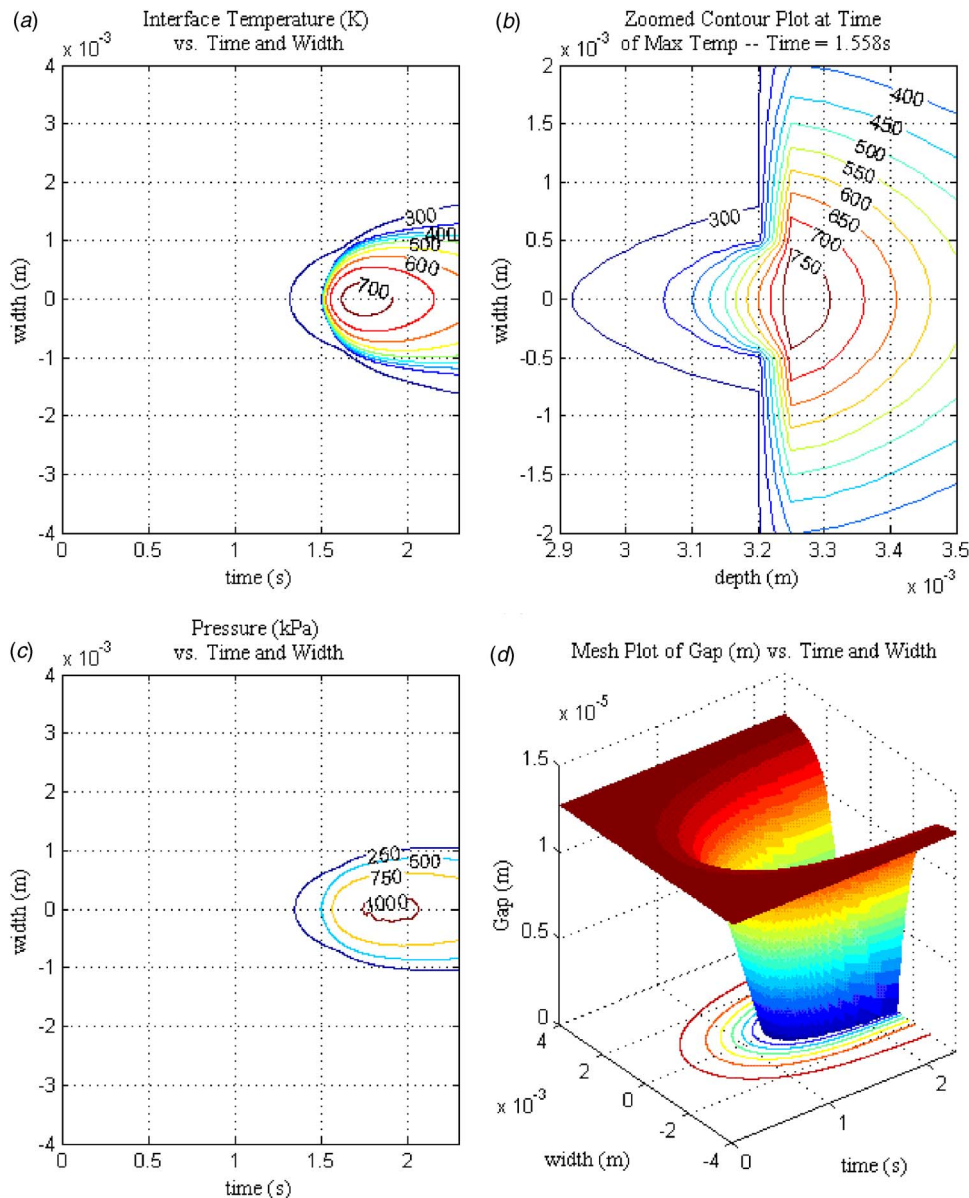


Fig. 2 The four output subplots of the model for the design solution bridging a $12.7 \mu\text{m}$ gap. Subplot (a) shows the temperature of the transmissive part at the interface of the two materials as a function of time and width. Subplot (b) is a zoomed contour plot of the interface zone at the time step that the maximum temperature occurs. In this case, the interface is at a depth $=3.2 \times 10^{-3}$ m. Subplot (c) shows the internal pressure as a function of time and width. Finally, subplot (d) shows the gap size along the width as a function of time. The width dimension is along the x axis (Fig. 1) with a mirror boundary condition at $x=0$. Note the large elapse time before the gap is closed and heating of the transmissive material begins.

width for this solution is 3.00 mm and again is defined as the width above 485 K. This larger width is primarily due to the larger laser beam diameter of 8 mm.

Experimental Setup

Modeling gap bridging with LTW has not been previously accomplished and thus the described model needs to be experimentally validated. A method was designed to create a known gap size in a T-joint geometry in a welding fixture. To create a known gap size, two short pieces of polyester shimstock are placed on top of the absorptive part at both ends outside of the weld zone. The transmissive part is then placed horizontally on the shims, creating the T-joint geometry with a known gap between the two parts, as

seen in Fig. 6. The assembled samples are placed in the welding fixture (Fig. 7) to secure the T-joint geometry and assure alignment with the laser during welding. A very minimal pressure of 50 kPa was applied to the sample to maintain contact from the transmissive part to the shims and from the shims to the absorptive part.

The laser system used for the welding experiments consists of a 30 W, 808 nm diode laser bar manufactured by Cutting Edge Optonics that is conductively cooled using a Peltier cooler. The diode bar is coupled to a 2 m long, 1.1 mm diameter fiber optic cable with an output lens assembly that is kept clear of dust and debris by a positive airflow nozzle. The laser spot diameter is adjustable between 2 mm and 10 mm by moving a slide that

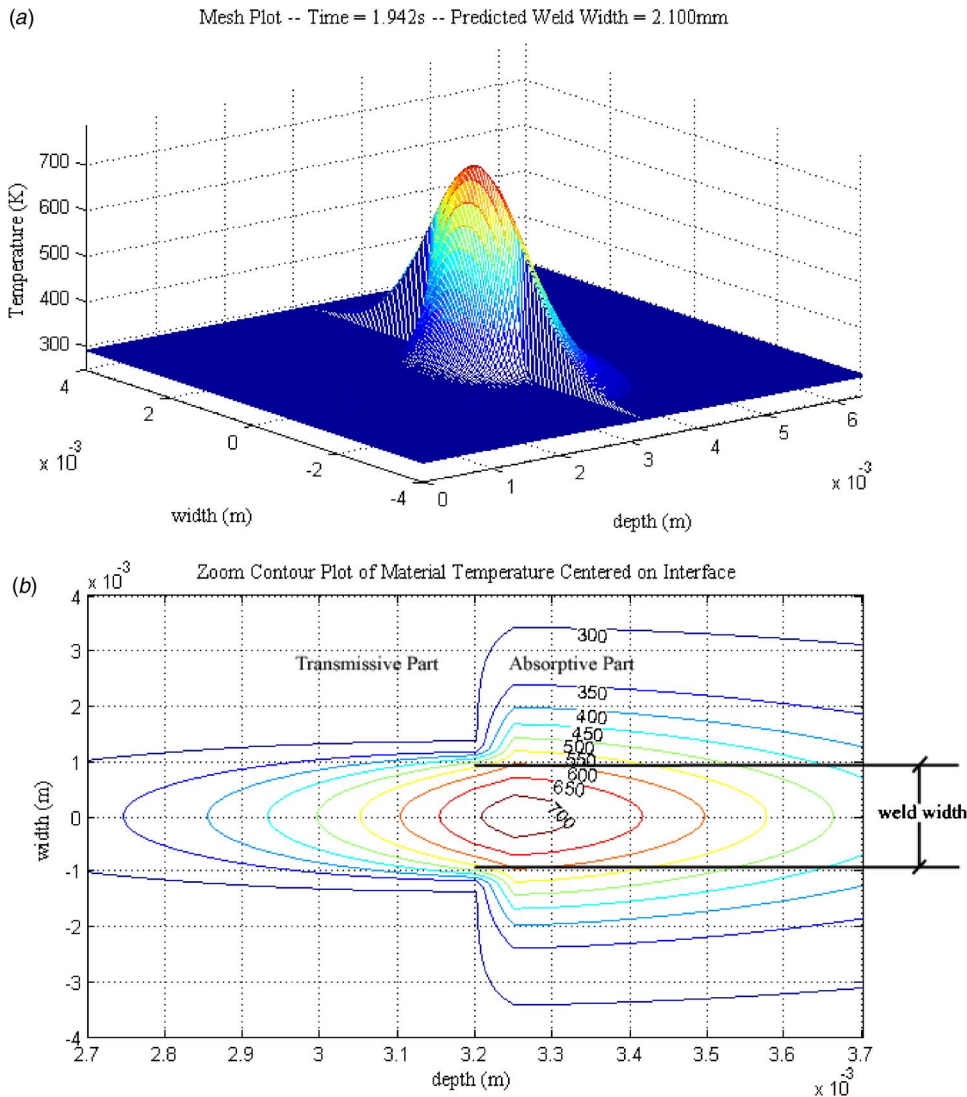


Fig. 3 Mesh and zoomed contour plots of the model bridging a $12.7\ \mu\text{m}$ gap. This frame coincides with the time the maximum weld width is reached. The interface between the two materials is at a depth $=3.2 \times 10^{-3}\ \text{m}$. Note the distinct temperature distribution difference between the absorptive and transmissive parts due to the large time elapse before heating in the transmissive part begins.

changes the distance between the optic head and the working surface. The laser is powered by a Kepco 2 V power supply that operates at up to 50 A.

Experimental Procedure

Using the above-described method of creating a gap in a T-joint geometry, five samples were welded at each gap size using the parameters from the model. Efforts were made to minimize sources of undesired variation in the experiment. PVC samples were sheared from large sheets into sizes slightly larger than the final dimensions. The samples were then machined to size in a manual vertical mill. Because the contact conduction is inversely proportional to the surface roughness, the variation in roughness cannot be overlooked. The surface roughness was measured with a Surtronic 10, manufactured by Taylor-Hobson. For this experiment, only samples with a measured roughness of $1.3\ \mu\text{m}$ were selected.

Prior to welding, the contacting surfaces of the “transparent” and the “absorptive” parts were cleaned with a cotton swab containing an isopropyl alcohol and water mixture. The purpose of

cleaning the surfaces is to remove any oil from handling or machining that might interfere with the integrity of the weld. The appropriate shims were put in place and the samples were inserted in the welding fixture. After welding, the parts were left in the fixture for 30 s. The reason for this extended holding period was to allow thorough cooling of the weld zone, necessitated by the longer heating time.

During welding, the laser system was run in a vector mode using the computer interface. In the vector mode, the laser optics head is initially 25 mm away from the weld zone. The optics head is then moved 10 mm away from the sample to allow an appropriate acceleration distance. Once the head has reached full velocity and crosses the original position, the laser begins to fire as the optics head continues to traverse across the weld zone. After crossing the weld zone, the power to the laser is interrupted and the optics head returns to the initial position. The purpose of starting the laser 25 mm away from the weld sample is to minimize the effect on any possible power spikes when first powering the laser.

The welded samples were assessed by three different measure-

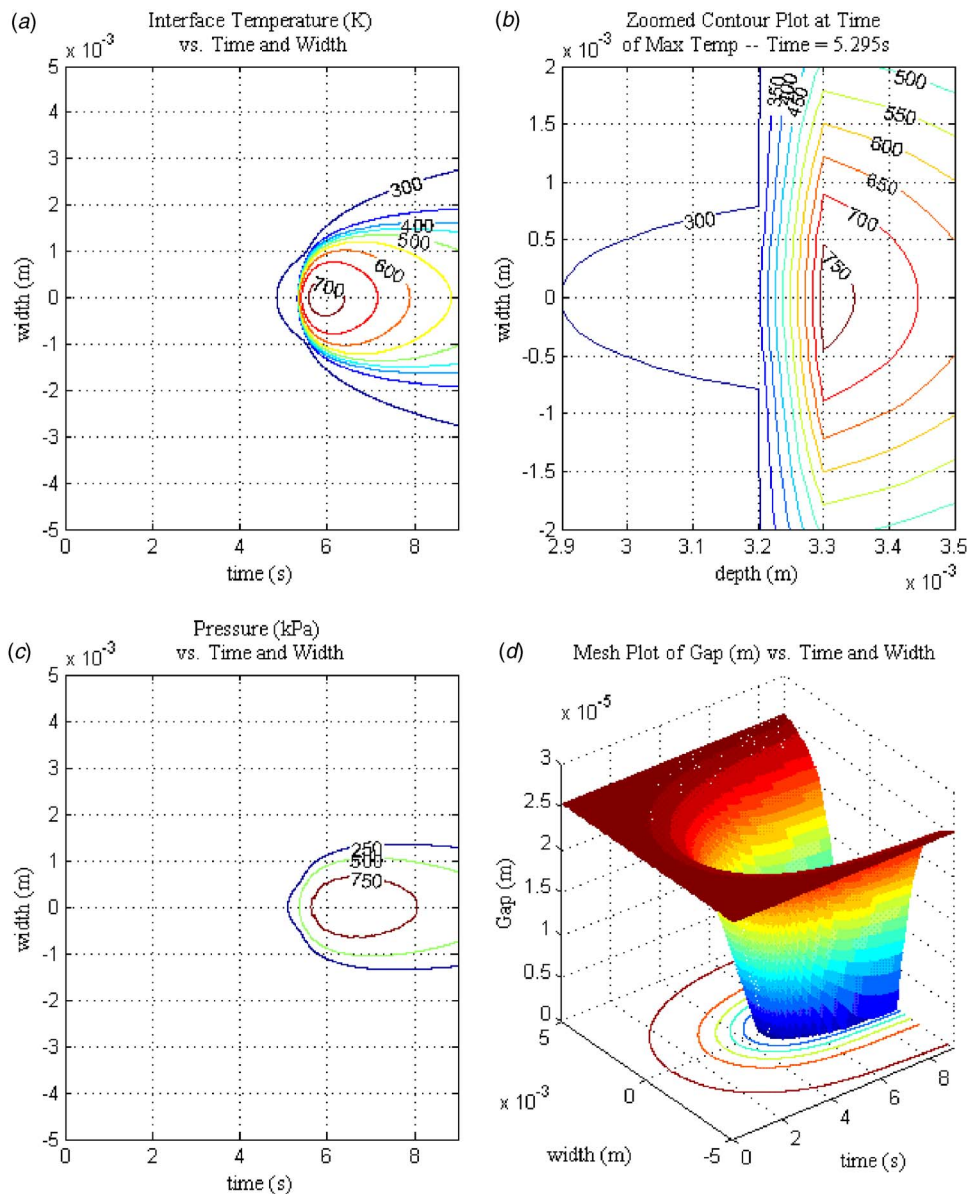


Fig. 4 Model outputs from the model for bridging a 25.4 μm gap. The operating conditions for this model include a laser power of 2.5 W, a welding velocity of 0.001 m/s, and a laser beam diameter of 8 mm. Note that the large time delay before the gap is closed and heating of the transmissive part begins.

ments. First, a qualitative visual inspection yielded information about weld width consistency and determined if visible thermal decomposition occurred. Welds were classified in one of the following manners: no weld, narrow weld, tapering weld, good weld, slight burn, moderate burn, or heavy burn. A “good” weld, which described the majority of samples in this experiment, is characterized by a uniform looking weld that shows no sign of thermal decomposition. The second assessment quantified the force required to fail the weld in a tensile test using a custom grip and fixture. Finally, the width of the weld was measured with a caliper, which allows calculation of the cross-sectional weld area and the failure strength.

The modeling discussed earlier in the paper predicts that the weld width for the 25.4 μm gap samples will be significantly larger than the 12.7 μm gap size due to the increase in the laser beam diameter. This increase in weld width requires more force per weld length to fail the weld. To assure that the pull force of the samples falls within the resolution of the load frame discussed

below, the weld length was adjusted for the two samples. The weld length for the 12.7 μm gap samples was set to 19 mm while the weld length was set to 11 mm for the 25.4 μm gap samples. The weld length was adjusted by changing the length of the opening window above the transparent part on the rotating carriage of the welding fixture.

A grip and fixture were designed to apply a tensile force to the weld samples in a loadframe. The top fixture is essentially an inverted “T slot” where the transmissive part slides into a horizontal slot, and the absorptive part extends vertically down out of the slot. The other end of the absorptive part is clamped in a simple grip that uses two socket head cap screws to apply a clamping force. Note that the weld width of these samples was not the full width of the stem of the *T*, resulting in stress concentration and peeling near the edges of the weld. These stress concentrations do affect the calculated weld strength.

An MTS electromechanical load frame was used for the de-

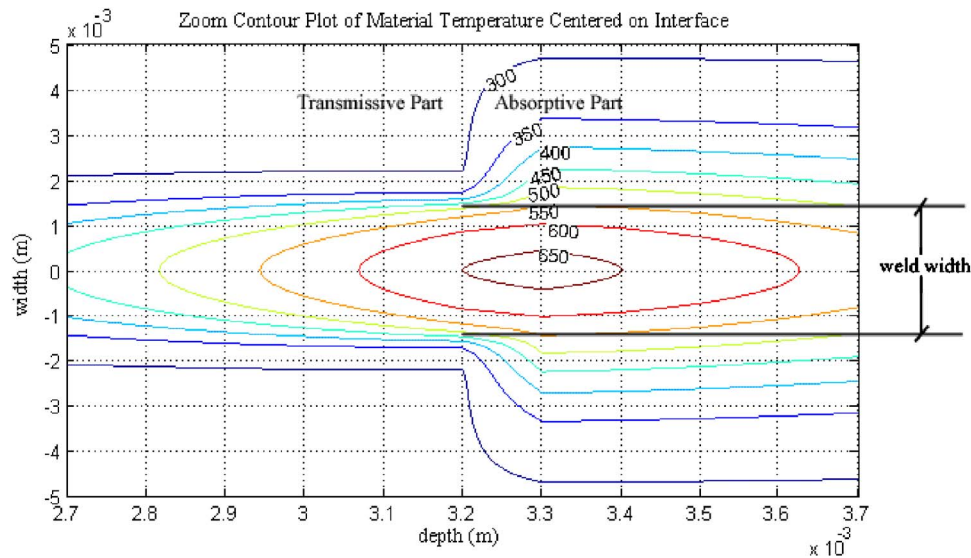


Fig. 5 A zoomed contour plot from the model bridging a $25.4 \mu\text{m}$ gap. The operating conditions for this model include a laser power of 2.5 W, a welding velocity of 0.001 m/s, and a laser beam diameter of 8 mm. The time step of this frame coincides with a maximum width for a 485 K temperature contour at the weld interface, which defines the weld width. The weld width predicted by this model is 3.00 mm. Note that the interface between the two parts is at a depth of 3.2 mm.

structive force testing. Samples were pulled in tension at a constant displacement rate of 1.25 mm/min using a 1000 N load cell. As discussed earlier, the weld length for the two different gap sizes was adjusted to be within the resolution of the available load cell.

Experimental Results

All five $12.7 \mu\text{m}$ gap samples bridged the gap and formed welds. Of these samples, four welds were given a rating of good through visual inspection, while the one sample showed slight decomposition along the centerline of the weld. The welds were pulled in tension to failure in the electromechanical load frame; the failure forces ranged from 565 N to 1001 N. Following the tensile test, the weld widths were measured and found to range from 2.49 mm to 2.54 mm. Finally, the weld strength was calculated by dividing the failure force by the area of the weld zone,

defined as the weld width multiplied by the 19 mm weld length, which ranged from 11.8 MPa to 20.7 MPa. These data for the $12.7 \mu\text{m}$ gap samples can be found in Table 1.

All five $25.4 \mu\text{m}$ gap samples formed welds across the gap and achieved a rating of good from the visual assessment. As with the previous gap size, the samples were assessed based on aesthetics, a destructive tensile test, and calculation of weld strength, which

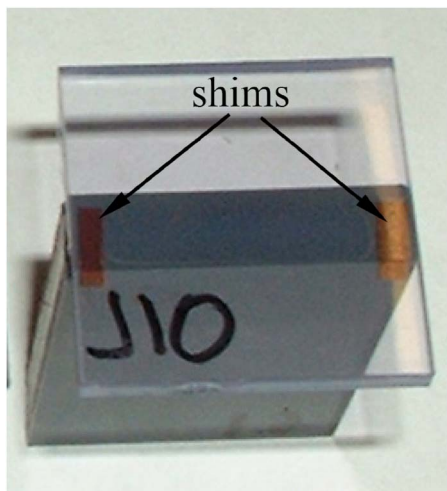


Fig. 6 The T-joint geometry shown with the two shims on either side of the weld zone. These shims establish the desired gap size.

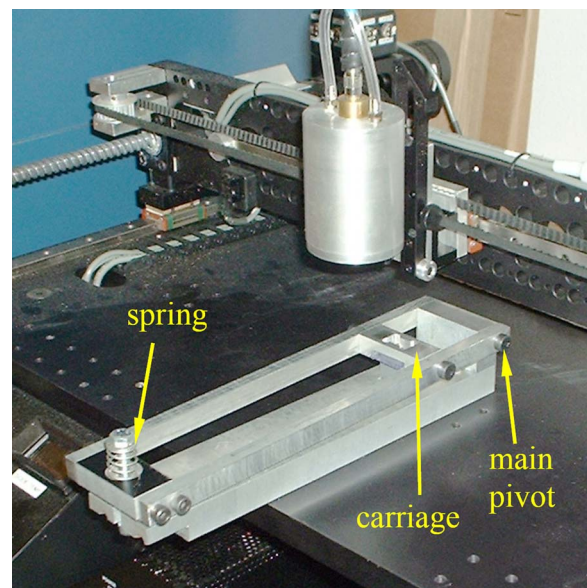


Fig. 7 Laser welding fixture mounted to the welding table. The arms pivot at the far right of the fixture. The absorbing part is placed in a slot approximately 50 mm from the first pivot. The shims are placed on the absorptive part followed by the transmissive part, forming the T-joint geometry. The transmissive part is held in place by a rotating carriage, which is the second pivot on the pair of arms. On the far left side of the arms, a precision spring is set to a very low force to only maintain light contact between the parts and not to compress the shims.

Table 1 The measured and calculated outputs from the five replications bridging a 12.7 μm gap

Trial	Visual rating	Failure force (N)	Weld width (mm)	Strength (MPa)
1	Slight decomposition	704.6	2.46	15.0
2	Good	1000.8	2.54	20.7
3	Good	705.5	2.49	14.9
4	Good	848.7	2.49	17.9
5	Good	564.9	2.51	11.8

are tabulated in Table 2. The failure force from the tensile test ranged from 367 N to 584 N. The weld width ranged from 4.22 mm to 4.24 mm. The calculated weld strength across the 11 mm long weld ranged from 7.9 MPa to 12.6 MPa.

Discussion

The experimental work above demonstrates that gaps can be bridged in LTW and that the operating parameters can be designed using a comprehensive two-dimensional modeling. The created welds were aesthetically pleasing, consistent across a small sample size, and had substantial failure strength. Note that despite efforts to minimize noise variables in the experiment, significant weld strength variation was found. This is likely due to the tensile test procedure, where slight misalignment in the grip and fixture can result in unequal loading of the weld. In comparison with operating without a gap, creating a successful weld across a gap requires the welding velocity to be drastically decreased to allow for thermal diffusion and the line energy to be decreased to prevent decomposition.

In previously described work [1,3], successful welds were formed at velocities up to 0.07 m/s (2.76 in./s) when no gap was present. This welding velocity could be further increased by increasing the laser intensity, which is defined by the laser power and beam diameter. As described in this paper, bridging a 12.7 μm (0.0005 in.) gap required the weld velocity to be decreased to 0.0025 m/s (0.10 in./s). To bridge a 25.4 μm (0.001 in.) gap, a further decrease in the laser velocity to 0.001 m/s (0.039 in./s) is required. The significant decrease in welding velocity is needed to allow time for heat diffusion to occur within the absorptive part. Previous work found that during high-velocity gap-free welding situations, the maximum temperature typically occurs slightly below the surface of the absorptive part, with a significant decreasing temperature gradient with increasing depth [1,2]. The longer weld times demonstrated in this paper decrease the temperature gradient and enable more of the absorptive material to expand, bridging the gap.

From the three assessment techniques of the welds formed across a gap, visual appearance, weld strength, and weld width, the overall outcome was quite positive. Visually, nine of the ten samples were given a visually good rating, while the other showed a slight area of decomposition along the centerline of the weld. The weld length for the two different gap sizes was different, to keep the required failure force within the capacity of the available load frame. While the failure forces cannot be compared directly due to these differences in weld area, the weld strength can be

Table 2 This table displays the measured outputs from five welding samples bridging a 25.4 μm gap

Trial	Visual rating	Failure force (N)	Weld width (mm)	Strength (MPa)
11	Good	480.9	4.24	10.3
12	Good	431.6	4.24	9.3
13	Good	466.6	4.22	10.1
14	Good	584.1	4.22	12.6
15	Good	367.0	4.22	7.9

compared. The average weld strength for the 12.7 μm samples is 16.1 MPa with a standard error of 1.5 MPa, while the average strength for the 25.4 μm samples is 10.0 MPa with a standard error of 0.8 MPa.

The agreement between the weld widths predicted by the model with the weld width achieved in the experiments was adequate, but not excellent. The width predicted for the 12.7 μm gap was 2.10 mm, while the average measured width was 2.50 mm, a 16% difference. The weld width predicted for the 25.4 μm gap was 3.00 mm, while the average measured width was 4.23 mm, a difference of 29%. These differences are most likely due to the thermal diffusion during the extended welding time. The model is a two-dimensional model, assuming that all the nodes in the modeled plane have an initial temperature equal to the ambient temperature. With long elapse times, the diffusion of heat within the polymer increases the temperature in all directions, including in the direction of laser travel. Thus, the initial temperature in the modeled area is actually higher than expected. For more accurate modeling of this situation, a three-dimensional model might be more appropriate.

Conclusion

In manufacturing applications, poor dimensional control can lead to the formation of gaps between mating part features requiring welding. Gaps in the weld joint create a significant problem for LTW because of the reliance on contact conduction between the absorptive and transmissive parts. Previous research has assumed gap-free joints.

This paper uses a previously constructed two-dimensional numerical model to design operating parameters for bridging gaps in LTW. In the design of parameters for a 12.7 μm gap and a 25.4 μm gap, the welding velocity and laser power needed to be decreased significantly compared to a gap-free joint. These changes are necessary to create heating into a sufficient depth of the absorptive part, which creates the thermal strain necessary to bridge the gap.

Experiments with a diode laser system used the designed operating parameters to create five welded samples of each gap size. All samples successfully bridged the gap and formed welds. Of the ten samples, nine achieved an aesthetic good rating, while one sample showed slight decomposition. Samples were also assessed by measuring the tensile force at failure in a load frame and the weld width. From these data, the weld strength was calculated and found to average 16.1 MPa for the 12.7 μm gap samples and 10.0 MPa for the 25.4 μm gap samples.

The weld width of the experimental samples adequately agreed with the predictions of the model. The difference between the measured width and the predicted width was 16% for the 12.7 μm gap samples and 29% for the 25.4 μm gap samples. This discrepancy is likely due to the large thermal diffusion occurring in all directions, including along the direction of the laser travel due to the long weld times. The numerical model is two-dimensional, which was demonstrated to successfully predict weld widths at higher welding velocities [1,3]. When bridging gaps, the elapse time is long enough that significant diffusion of the absorbed radiation occurs, heating the regions in front of the laser path. As the laser travels along the path, the area being irradiated is at a higher initial temperature, which results in a wider weld than predicted. This concept is supported by the fact that the error in the predicted weld width is greater for the 25.4 μm trial, which required a longer elapse time. While more computationally intensive, a three-dimensional model would be more accurate in simulating bridging gaps in LTW. For a rough estimation of operating parameters, the two-dimensional model provides adequate results.

Acknowledgment

The authors would like to thank Andersen Corporation for generously sponsoring this work.

References

- [1] Van de Ven, J., 2006, "Laser Transmission Welding of Thermoplastics," thesis, University of Minnesota, Minneapolis.
- [2] Van de Ven, J., and Erdman, A., 2007, "Laser Transmission Welding of Thermoplastics—Part I: Temperature and Pressure Modeling," ASME J. Manuf. Sci. Eng., in press.
- [3] Van de Ven, J., and Erdman, A., 2007, "Laser Transmission Welding of Thermoplastics: Part II: Experimental Model Validation," ASME J. Manuf. Sci. Eng., in press.
- [4] Russek, U. A., Palmen, A., Staub, H., Pohler, J., Wenzlau, C., Otto, G., Poggel, M., Koeppe, A., and Kind, H., 2003, "Laser Beam Welding of Thermoplastics," Proc. SPIE, **4977**, pp. 458–472.
- [5] Abu-Sharkh, B. F., 2001, "Glass Transition Temperature of Poly(vinylchloride) From Molecular Dynamics Simulation: Explicit Atom Model Versus Rigid CH₂ and CHCl Groups Model," Comput. Theor. Polym. Sci., **11**(1), pp. 29–34.
- [6] Van de Ven, J., and Erdman, A., 2006, "Near-Infrared Laser Absorption of Polyvinylchloride at Elevated Temperatures," J. Vinyl Addit. Technol., **12**(4), pp. 166–173.
- [7] Povoio, F., Schwartz, G., and Hermida, E. B., 1996, "Stress Relaxation of PVC Below the Yield Point," J. Polym. Sci., Part B: Polym. Phys., **34**, pp. 1257–1267.
- [8] Collins, E. A., Daniels, C. A., and Witenhafer, D. E., 1999, *Polymer Handbook*, Wiley, New York.
- [9] Fuller, J. J., and Marotta, E. E., 2001, "Thermal Contact Conductance of Metal/Polymer Joints: An Analytical and Experimental Investigation," J. Thermophys. Heat Transfer, **15**(2), pp. 228–238.
- [10] Cengel, Y. A., 1998, *Heat Transfer: A Practical Approach*, 3rd. ed., McGraw-Hill, Boston, p. 1006.
- [11] Van de Ven, J., and Erdman, A., 2006, "Hot Pin Welding of Thin Polyvinyl Chloride Sheet," J. Vinyl Addit. Technol., **13**(2), pp. 110–115.
- [12] Goings, J., 2005, "Cutting Edge Optronics," St. Charles, MO. Data Sheet on Laser Diode Array SN27983.